Proceedings of 2013 IAHR Congress
© 2013 Tsinghua University Press, Beijing

A Hydraulic Roughness Model for Submerged Flexible Vegetation

Afis Olumide Busari
Research Student, Department of Civil and Environmental Engineering, The Hong Kong Polytechnic University, Hong Kong, China. Email: mscbusari@gmail.com

Chi-wai Li,
Professor, Dept. of Civil and Environmental Engineering , The Hong Kong Polytechnic University, Hong Kong, China.E-mail: cecwli@polyu.edu.hk

ABSTRACT: Submerged vegetation is a key component in natural and restored rivers. It preserves the ecological balance yet has a hydraulic impact on the flow carrying capacity. The hydraulic resistance produced by submerged flexible vegetation depends on many factors, including the vegetation stem size, height, number density and flow depth. In the present work a numerical model is used to generate synthetic velocity profile data for hydraulic roughness determination. In the model turbulence is simulated by the Spalart-Allmaras closure with a modified length scale which is dependent on the vegetation density and vegetation height to water depth ratio. Flexibility of vegetation is accounted for by using a large deflection analysis. The model has been verified against available experiments. Based on the synthetic data an inducing equation is derived, which relates the Manning roughness coefficient to the vegetation parameters, flow depth and a zero-plane displacement parameter.

KEY WORDS: Flexible vegetation, Hydraulic roughness, Inducing equation, Zero-plane displacement.

1 INTRODUCTION

Submerged vegetation is a key component in natural and restored rivers. The ongoing promotion of the natural development of wetlands and other restoration projects to enhance development within river basins favors the growth of submerged vegetation. Vegetation preservation is of great significance to the ecological balance yet has a hydraulic impact on the flow carrying capacity. The hydraulic resistance produced by submerged flexible vegetation depends on many factors, including the vegetation stem size, height, number density and flow depth.

Carollo et al. (2005) reported that the application of the well-known Kouwen's method overestimated the flow resistance in an open channel with flexible vegetation. The coefficients in the logarithmic equation of flow resistance were subsequently recalibrated against their experimental data. It was analyzed dimensionally that at high vegetation density, the shear Reynolds number has to be included in the flow resistance law. Järvelä (2005) investigated experimentally the flow resistance above flexible vegetation in an open channel flume using Acoustic Doppler Velocimetry technique and confirmed that the logarithmic velocity profile for smooth open channel flow is altered in vegetated flow and the Darcy-Weisbach's friction factor can be related to the maximum shear stress which occurs approximately at the deflected plant height.

Wilson, (2007) investigated the variation of hydraulic roughness parameters with flow depth and found that the Manning roughness coefficient increases with decreasing flow depth reaching an asymptotic constant at high submergence depth ratio (water depth to vegetation height). The value of the constant is dependent on the vegetation height and other vegetation properties. Baptist et al. (2007)

proposed three equations describing the vegetation induced resistance from different angles. Two equations were based on analytical approach, and one equation was based on analyzing of the synthetic data generated by a 1-D k-ε model using the genetic programming approach.

Nikora et al, (2008) studied the impacts of vegetation on hydraulic resistance and suggested simple quantitative relation to predict these effects based on flow and vegetation parameters. The analysis showed that the submergence depth ratio was the major parameter to determine hydraulic roughness. Takaaki and Nezu, (2010) examined experimentally the flow structure in an open channel flow with flexible vegetation and confirmed that the zero plane displacement is well correlated with the plant deflected height and that the friction factor increases with the deflected height. Therefore, the mean deflected height was suggested to be a key parameter for hydraulic roughness.

In the present work the numerical modeling approach is used to generate synthetic velocity profile data for hydraulic roughness determination. In the model turbulence is simulated by the Spalart-Allmaras closure with a modified length scale which is dependent on the vegetation density and water depth to vegetation height ratio. Flexibility of vegetation is accounted for by using a large deflection analysis. The model is verified against available experiments. Based on the synthetic data an inducing equation is derived, which relates the Manning roughness coefficient to the vegetation parameters, flow depth and a zero-plane displacement parameter. The derived equation is compared with an existing equation, as well as the data sets of flume experiments conducted by various researchers. Finally the predictive capability of the derived equation is tested in field conditions.

2 NUMERICAL MODEL

The numerical model for the determination of hydraulic roughness is based on conservation of mass and momentum of fluid.

Continuity equation:

$$\frac{\partial u_i}{\partial x_i} = 0 \qquad i=1,2,3 \tag{1}$$

Momentum equation:

$$\frac{\partial u_i}{\partial t} + u_j \frac{\partial u_i}{\partial x_j} = \frac{\partial}{\partial x_j}\left[\nu_m\left(\frac{\partial u_i}{\partial x_j} + \frac{\partial u_j}{\partial x_i}\right) + \frac{\tau_{ij}}{\rho}\right] - \frac{1}{\rho}\frac{\partial p}{\partial x_i} - \frac{1}{\rho}F_i + g_i \qquad i=1,2,3 \tag{2}$$

where x_i (= x, y, z) are the coordinates in longitudinal, transverse and vertical directions respectively; u_i (= u, v, w) are the time-averaged velocity components in x, y and z directions respectively; t =time; ρ=density of fluid; ν_m=molecular viscosity, $\tau_{ij} = -\rho\overline{u_i' u_j'}$ =Reynolds stresses, F_i ($= F_x$, F_y, F_z) are the resistance force components per unit volume induced by vegetation in x, y and z directions respectively. g_i (=0, 0, -9.81m/s^2) are the components of the gravitational acceleration. The Reynolds stresses are represented by the eddy viscosity model:

$$\frac{\tau_{ij}}{\rho} = -\overline{u_i' u_j'} = \nu_t\left(\frac{\partial u_i}{\partial x_j} + \frac{\partial u_j}{\partial x_i}\right) - \frac{2}{3}\delta_{ij}k \tag{3}$$

where $k = \frac{1}{2}\overline{u_i' u_i'}$ is the turbulent kinetic energy which can be absorbed into the pressure gradient term,

ν_t =eddy viscosity. The eddy viscosity ν_t is specified by the Spalart-Allmaras (SA) turbulence model which involves the solution of a new eddy viscosity variable ν. The version of the model used is for near-wall region and finite Reynolds number, which is most relevant to the present problem (Spalart and Allmaras, 1994).

$$\frac{\partial \nu}{\partial t} + u_j \frac{\partial \nu}{\partial x_j} = c_{b1}\tilde{S}_\nu \nu + \frac{1}{\sigma}\left\{\frac{\partial}{\partial x_j}\left[(\nu + \nu_m)(\frac{\partial \nu}{\partial x_j})\right] + c_{b2}\left(\frac{\partial \nu}{\partial x_j}\frac{\partial \nu}{\partial x_j}\right)\right\} - c_{w1}f_w\left(\frac{\nu}{d}\right)^2 \tag{4}$$

where

$$\nu_t = \nu f_{v1}, \quad \tilde{S}_\nu = S_\nu + \frac{\nu}{\kappa^2 d^2} f_{v2}, \quad S_\nu = \sqrt{\omega_j \omega_j}, \quad \chi = \frac{\nu}{\nu_m}$$

$$f_{v1} = \frac{\chi^3}{\chi^3 + c_{v1}^3}, \quad f_{v2} = 1 - \frac{\chi}{1 + \chi f_{v1}}, \quad f_w = g\left[\frac{1 + c_{w3}^6}{g^6 + c_{w3}^6}\right]^{1/6}$$

$$g = r + c_{w2}(r^6 - r), \quad r = \frac{\nu}{\tilde{S}_\nu \kappa^2 d^2}$$

$S_\nu = \sqrt{\omega_j \omega_j}$ = magnitude of the vorticity, κ=0.41, σ=2/3, c_{b1}=0.1355, c_{b2}=0.622, c_{v1}=7.1, $c_{w1} = \frac{c_{b1}}{\kappa^2} + \frac{1 + c_{b2}}{\sigma}$, c_{w2}=0.3, c_{w3}=2, d=length scale, S_F=additional source term due to vegetation. This turbulence model is a one-equation model which is simpler than the commonly used k-ε or k-ω model and it has been successfully applied in the modelling of certain free-shear flow, wall-bound flow and separated flow problems. The resistance force due to vegetation is determined by the quadratic friction law. The average force per unit volume within the vegetation domain is obtained by

$$F_i = \frac{1}{2}\rho C_D b_v N u_i \sqrt{u_j u_j} \qquad i=1,2 \tag{5}$$

where C_D=drag coefficient of stem, b_v=width of stem and N=vegetation density ($1/m^2$) .

For wall bounded shear flow, the turbulence length scale d is proportional to the distance from the point of interest to the channel bed. In the presence of vegetation, the turbulence eddies above the vegetation canopy may not reach the channel bed and thus the turbulence length scale will be reduced. One approach to model the reduction in the turbulence length scale is to set a zero plane displacement parameter z_0. The proposed turbulence length scale of a point at level z is given by

$$L = z - z_0 \qquad z > k > z_0$$
$$L = z(k - z_0)/k \qquad z < k \tag{6}$$

where k=deflection vegetation height.

Natural vegetation bends in high flow and the horizontal deflection at the top of a vegetation stem can be of the same order as the deflected stem height. Hence, the classical small deflection theory of a beam may not be adequate for a vegetation stem with high flexibility. In this work, a large deflection analysis based on the Euler-Bernoulli law for bending of a slender beam has been used to describe the deflection of a vegetation stem (Li and Xie, 2011). In the analysis each vegetation stem is modeled as a vertical in-extensible non-prismatic slender beam of length l. The water flow produces variable distributed loads $q_x(s)$ on the beam along the *x*-direction as shown in Fig. 1. Combining the Euler-Bernoulli law for the local bending moment and the equations of the equilibrium of forces and moments, the following fourth order nonlinear equation in the deflection δ is obtained.

$$\frac{d^2}{ds^2}\left[EI(s)\frac{\frac{d^2\delta}{ds^2}}{1-\left(\frac{d\delta}{ds}\right)^2}\right]+\frac{d}{ds}\left[EI(s)\frac{\frac{d^2\delta}{ds^2}}{1-\left(\frac{d\delta}{ds}\right)^2}\right]\frac{\frac{d\delta}{ds}\frac{d^2\delta}{ds^2}}{1-\left(\frac{d\delta}{ds}\right)^2}=-q_x(s)\sqrt{1-\left(\frac{d\delta}{ds}\right)^2} \tag{7}$$

where s = local ordinate along the beam, E = flexural stiffness (N/m^2), I = second moment of area (m^4) and δ= deflection in *x*-direction. The vegetation stem is taken as inextensible as the total length remains constant. By dividing the stem into n equal part of constant length Δs, the z-ordinate of the ith node is obtained by

$$z_i=\sum_{j=1}^{i}\sqrt{\Delta s^2-(\delta_i-\delta_{i-1})^2} \tag{8}$$

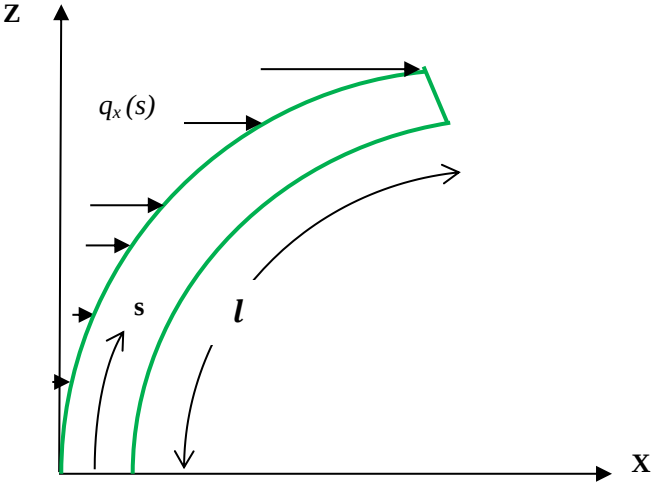

Figure1: Schematic diagram of large deflection of a beam carrying distributed load.

The deflected height of the stem is then equal to z_n. Eq. (7) is solved by using a quasi-linearized central finite difference scheme. To save computational effort, the solution is expressed in non-dimensional form relating the deflected height to the applied force, and is approximated by a polynomial. Details can be found in Li and Xie (2011).

Under uniform flow condition, the problem becomes one-dimensional and the 1D version of the numerical model by Li and Zeng (2009) can be used. The flow variables are the longitudinal velocity component u_1 and the eddy viscosity, varying along the vertical direction. The boundary conditions are as

follows. At the free water surface the normal gradients of the variables are zero. At the bottom the velocity is determined by the wall function and the eddy viscosity is determined by the mixing length hypothesis.

3 MODEL VERFICATION

Three cases have been chosen for the verification of the numerical model. The flow and vegetation parameters for the experiments are shown in Table 1. The number of grids used is 61 and the time step size is in the order of 0.0005s to ensure computational stability. Grid convergence study shows that further reduction of grid size does not affect the results apparently.

Table 1 Flow and vegetation parameters

Investigator(s)	Run	$N(m^{-2})$	h(m)	k(m)	$EI(Nm^2)$	U_m(m/s)	S(%)
Lopez and Garcia (2001)	Expt 1	142	0.335	0.12	Rigid	0.876	0.36
Jarvela (2005)	R4-8	12,000	0.707	0.280	$4.35x10^{-5}$	0.129	0.02
	R4-9	12,000	0.704	0.280	$4.35x10^{-5}$	0.185	0.03
Wilson (2007)	A-2	833,333	0.0480-0.165	0.016	-	0.139-0.343	0.1

h=water depth, U_m=mean velocity, S=channel bottom slope

Fig. 2 shows the comparison between the numerical results and the experimental data of Lopez and Garcia (2001). The computed velocity profile above the vegetation layer agreed well with that reported in the experiment and is more accurate than that computed by the k-ε turbulence model proposed by Lopez and Garcia (2001). The difference between the presently computed velocity above vegetation and the corresponding measured value is less than 7%.

The computed and measured velocity profiles for the cases of Wilson (2007) are shown in Fig. 3. The flexibility of the grass was not determined in the experiments. In the numerical simulation the flexural rigidity of grass was calibrated to reproduce the observed deflected height. The profile is in non-dimensional form and is obtained by combining the results of several experiments with different h/k ratios. The computed results and measured data are almost overlapping. The results show a good correlation of the trend of variation of the velocity with h/k ratio within the range of selected water depth.

Fig. 4 displays the computed and measured velocity profiles for the case of Jarvela (2005). The shear velocity is defined using the clear water depth (equal to total water depth minus the vegetation height), which is the same as that adopted by Jarvela (2005). The computed results are in good agreement with the measured data in the clear water zone and exhibit a low velocity region in the vegetation layer. There was no data recorded within the vegetation region, primarily due to the high vegetation density.

The vegetation induced roughness can be expressed in terms of the Manning coefficient through the Manning equation for uniform flow. The capacity of the numerical model in predicting the vegetation induced roughness effect is examined in 117 cases with available experimental data. The data were measured in laboratory flumes, covering a considerable range of vegetation parameters and flow depths, and were reported in six independent literatures (Ikeda, 1996; Poggi, 2004; Jarvela, 2005; Carollo et al., 2005; Velasco et al., 2010 and Zeng, 2011). In the computations, for cases in which the drag coefficient is not specified, the value of 1.2 is adopted. If the deflected height of vegetation is not specified, it will be computed using the large deflection analysis described above. The zero-plane displacement has been fine tuned to give the best fit result. The values of the Manning coefficient derived from the experimental data are compared with the calculated values using the model. As shown in Fig. 5, the agreement between the computed values and the measured data is good, with the difference generally within 10%.

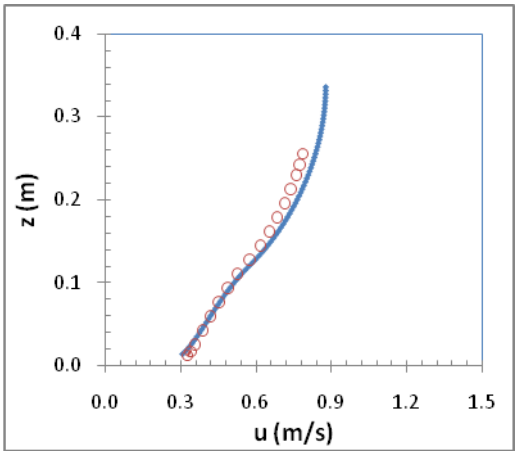

Figure 2: Velocity profile comparison for Lopez and Garcia (2001). Solid line – computed; circle – measured.

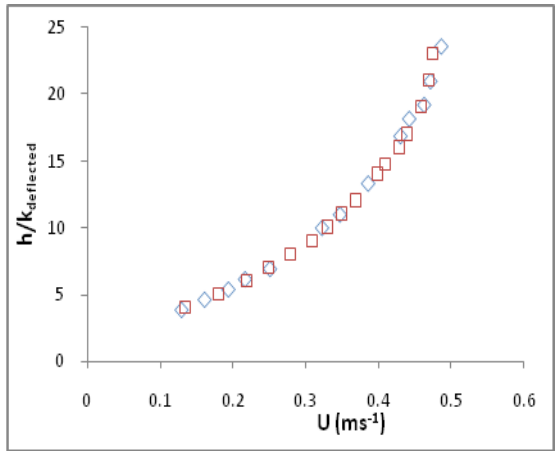

Figure 3: Velocity profile comparison for Wilson (2007). Rhombus –computed; square – measured.

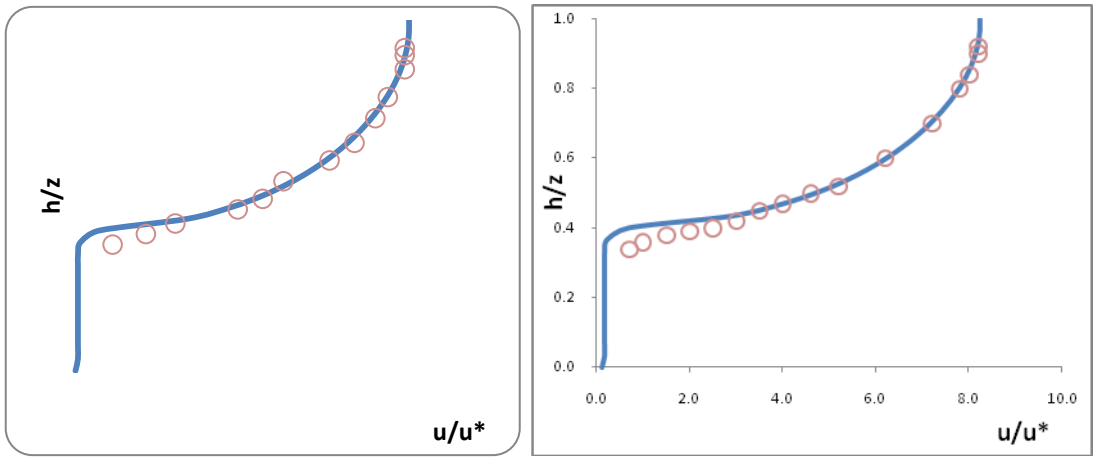

Figure 4: Velocity profile comparison for Jarvela (2005). Run R4-8 (left), Run R4-9 (right). Solid line –computed; circle – measured

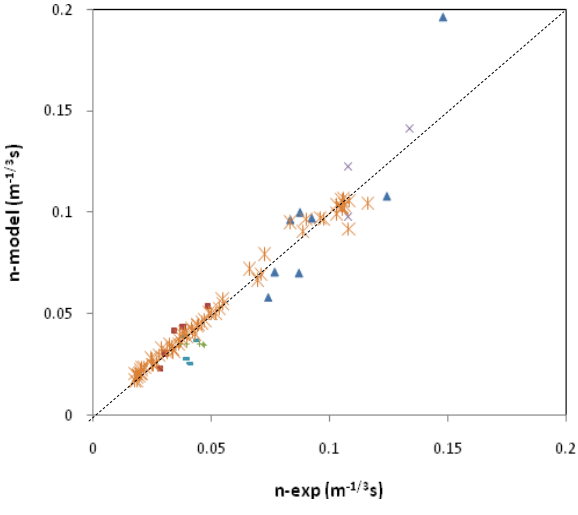

Figure 5: Comparison between the Manning coefficients determined from experiments and model simulations.
+Ikeda & Kanazawa (1996); □ Poggi et al. (2004); △Jarvela (2005); ∗ Carollo et al. (2005); −Velasco et al. (2010); × Zeng (2011)

4 INDUCING EQUATION

4.1 Fitting Equation

Numerical experiments have been carried out against available experimental data to obtain an empirical equation of z_0 which is given by

$$\frac{z_0}{h_v} = \frac{f_v^{\beta}}{f_v^{\beta} + \alpha^{\beta}} \tag{9}$$

where $f_v = Nb_v k$, α=0.5, β=0.7. The equation is in reasonable agreement with the equation proposed by Raupach (1994).

Several empirical equations for vegetation induced roughness have been proposed previously, including Kouwen and Unny (1973) for flexible vegetation, Baptist et al. (2007) and Gu (2007) for rigid vegetation. The equations are of the following general form.

$$n = \frac{h^{1/6}}{\sqrt{g}[a + b\log(h/k_s)]} \tag{10}$$

where a, b are parameters dependent on the flow and vegetation parameters; k_s is a roughness parameter. In the present work a refined empirical equation for vegetal roughness is derived from the numerical model generated synthetic data and will be compared with the other available equations. After extensive tests the following equation is proposed.

$$n = \frac{h^{1/6}}{\sqrt{\frac{2g}{f_v} + A'\frac{\sqrt{g}}{\kappa}\ln\left(\frac{h - z_0'}{k - z_0'}\right)}} \tag{11}$$

where A' is an empirical parameter and κ=0.41. The parameter, Z_o' represents a modified zero plane displacement parameter and is given by

$$z_0' = z_0 \exp\left(\frac{-\eta}{f_v^{3/4}}\right) \tag{12}$$

where η=3.7. Numerical simulations show that the parameter A' is a nonlinear function of h/k. The fitting of eq. (12) to the synthetic data from numerical simulations leads to the following quartic polynomial equation.

$$A'\left(\frac{h}{k}\right) = a_1\left(\frac{h}{k}\right)^4 + a_2\left(\frac{h}{k}\right)^3 + a_3\left(\frac{h}{k}\right)^2 + a_4\left(\frac{h}{k}\right) + 0.6026 \tag{13}$$

where a_1, a_2, a_3 and a_4 are constants equal to 0.0043, -0.0608, 0.2550 and -0.1604 respectively. The correlation coefficient of the fitting is high and is equal to 0.991. Fig. 6 shows that the fitting is the best at lower values of h/k, and has larger discrepancy when f_v is low and h/k is high (i.e. in the low hydraulic resistance range).

A simplified form of equation (11) can be obtained by noting that the exponential function in equation (12) approaches 1 at very high vegetation density ($f_v \to \infty$). In that case $z_o' \to z_0$, and equation (11) takes the following form:

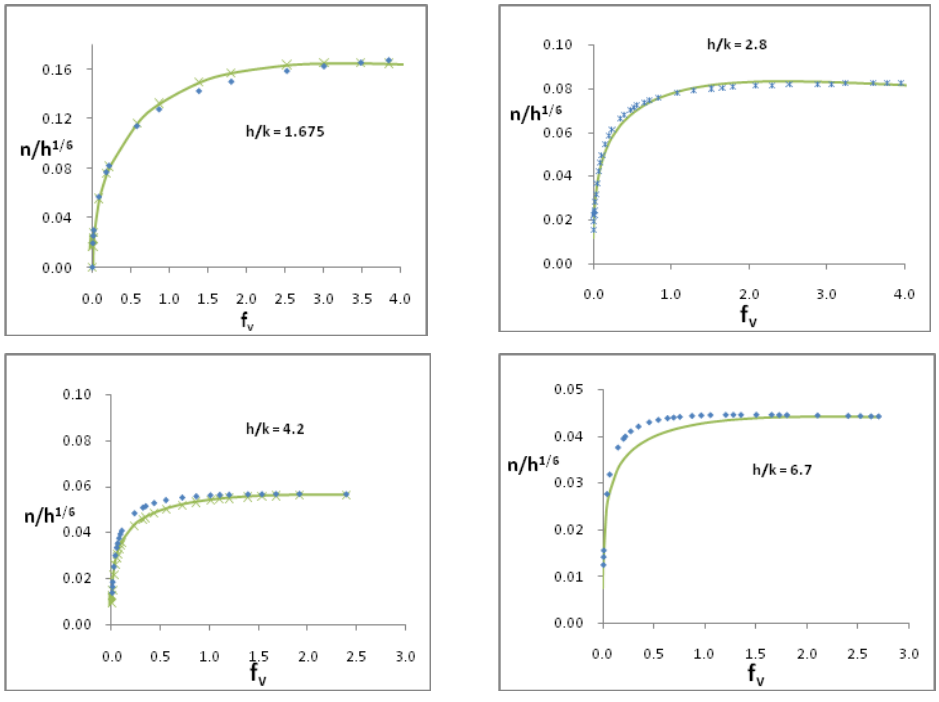

Figure 6: Fitting equation (11) and synthetic data for different submergence ratio. Dot – synthetic data; solid line – fitting equation

$$n = \frac{h^{1/6}}{\sqrt{\frac{2g}{f_v}} + A\frac{\sqrt{g}}{\kappa}\ln\left(\frac{h - z_0}{k - z_0}\right)} \tag{14}$$

The fitting of equation (14) to the synthetic data yields a quadratic polynomial equation of A and h/k with correlation coefficient approximately equal to 1. The equation is given by:

$$A\left(\frac{h}{k}\right) = b_1\left(\frac{h}{k}\right)^2 + b_2\left(\frac{h}{k}\right) + 0.3951 \tag{15}$$

where b_1 and b_2 equal to 0.0165 and 0.0379 respectively.

4.3 Verification of Equations

Eqs. (11) and (14) are then verified by the experimental data and compared with the equation proposed by Baptist et al (2007). The available experiments are subdivided into three categories with different vegetation densities. A brief description of the parameters of the data sets is shown in Table 2. In parallel the inducing equation by Baptist et al. (2007) is also employed for comparison. The equation is as follow and is simpler than Eqs. (11) and (14), but the zero plane displacement parameter is not included.

$$n = \frac{h^{1/6}}{\sqrt{\frac{2g}{f_v}} + \frac{\sqrt{g}}{\kappa}\ln\left(\frac{h}{k}\right)} \tag{16}$$

Table 2: A list of the datasets used in model verification

Investigator(s)	Category	m(m^{-2})	h/k	Vegetation Characteristics
Lopez and Garcia (2001) Huai et al. (2009) Velasco et al. (2010) Zeng (2011)	I	≤ 500	1.2≤ h/k ≤3.5	Artificial, rigid wooden dowels. Artificial, rigid metal rods. Artificial, flexible plastic strips. Artificial, flexible plastic strips.
Ikeda and Kanazawa (1996) Poggi et al. (2004) Jarvela (2005)	II	≤ 15,000	1.4≤ h/k ≤ 5.0	Artificial, flexible Nylon filaments. Artificial, rigid stainless steel. Natural, flexible wheat.
Carollo et al. (2002) Carollo et al. (2005)	III	≥20,000	1.6≤ h/k ≤ 9.0	Natural, flexible Barley grass. Grass mixture.

For category I in which the vegetation density is low, the vegetation is artificial and is either rigid or flexible. The comparison results are presented in Fig. 7, showing good agreement between the empirical equations and the experimental data. Eq. 11 gives the best fit results.

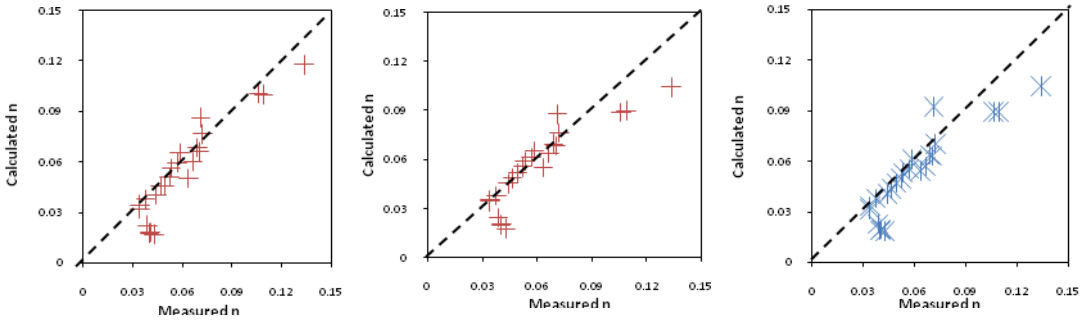

Figure 7: Comparison between the measured values of n ($m^{-1/3}s$) and those calculated using equation 11 (Left), equation 14 (Middle) and equation 16 (Right) for Category I cases

Category II consists of data corresponding to natural or artificial vegetation with medium density and wider range of degree of submergence. The results in Fig. 8 show that the equations generally yield good results comparing with the experimental data. Eq. 16 overestimates the Manning roughness at higher vegetation density whereas Eq. 14 produces wider scattering of the results around the line of perfect agreement.

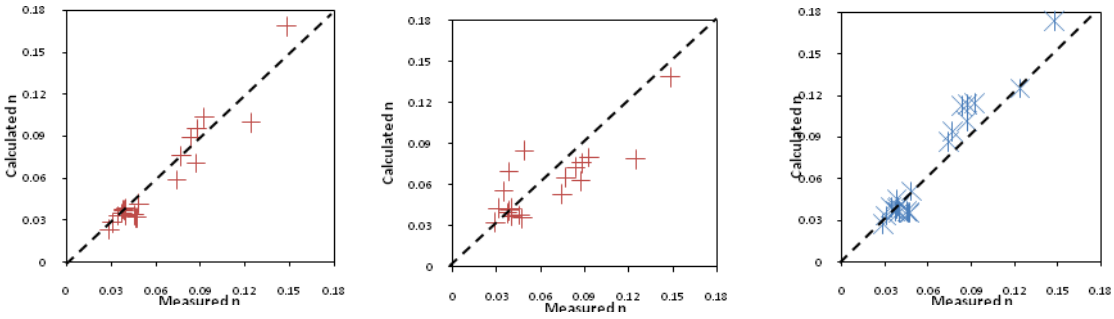

Figure 8: Comparison between the measured values of n ($m^{-1/3}s$) and those calculated using equation 11 (Left), equation 14 (Middle) and equation 16 (Right) for Category II cases

In category III the vegetation is natural and of very high density, ranging from 28,000 to 44,000 stems/m^2. In the simulation it was found that the drag coefficient needed to be adjusted to 0.1 due to the large deflection of the plants and the significant sheltering effect induced. Fig. 9 shows that the results computed by Eqs. 11 and 16 bias on the high side and overestimate the Manning's roughness coefficient. The degree of scatter increases with decreasing Manning roughness coefficient. Eq. 14 however gives good prediction results. This is mainly because the zero plane displacement z_0 is important for these cases with high vegetation density. Water flow is significantly retarded by the vegetation and the turbulence eddies cannot penetrate into the lower vegetation region. Eq. 14 is most sensitive to the change in z_0.

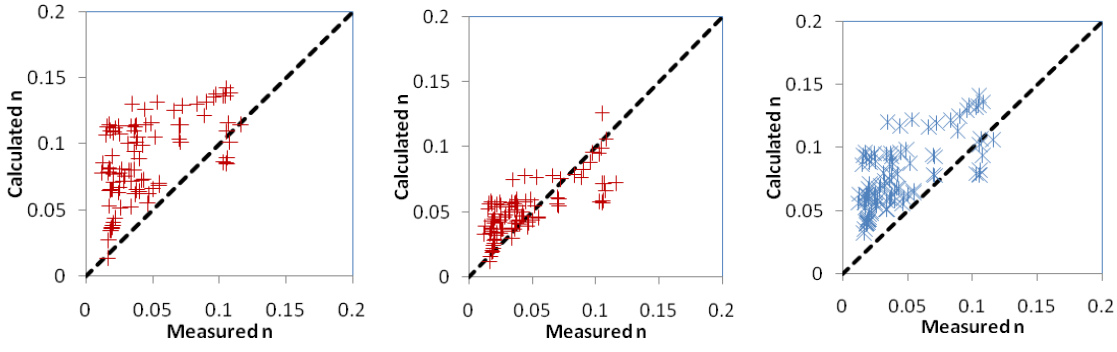

Figure 9: Comparison between the measured values of n ($m^{-1/3}s$) and those calculated using equation 11 (Left), equation 14 (Middle) and equation 16 (Right) for Category III

4.3 Field Application

While most empirical equations were validated against laboratory measurement data only (e.g. Klopstra et al, 1997; Stephan and Gutknecht, 2002; Brian et al., 2002, Gu, 2007 and Baptist et al, 2007), the present study extends the validation study against existing field data. Nikora et al, (2008) studied the impacts of aquatic vegetation on hydraulic resistance in five small streams and suggested empirical equations to predict these effects. The reach length of stream considered varied from 12 to 30m. The dominant vegetation types of varying flexibility and variable morphology under consideration were

Charophytic alga (Nitella hookeri), Myriophyllum sp., Riccia sp., Filamentous algae and Elodea canadensis.

In the simulation the parameter f_{rk} ($=C_D b_v N$) is not available and needs to be estimated. The drag coefficient C_D is in the order of 1, the exact value depends on the streamlined flow effect due to vegetation deflection. The stem width b_v lies between 4-6mm and the density N depends on the plant characteristics (Bowmer et al, 1995; Hofstra et al, 2006; Kevin et al, 2007). In the simulation, the average stem width is taken to be 5mm for all vegetation types, the vegetation density is assumed to be 12,000/m^2. Fig. 10 shows that the computed Manning's coefficients are in good agreement with the measured data reported by Nikora et al. (2008). The predicted value of the Manning's coefficient is found not quite sensitive to the value of f_{rk} within the practical range.

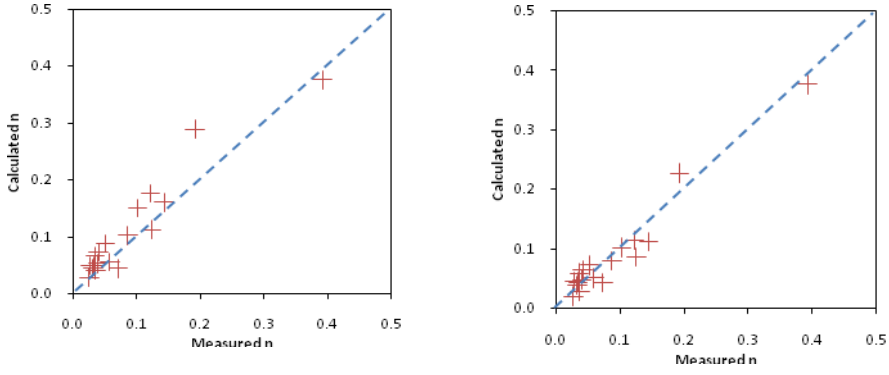

Fig. 10: Field verification of Eq. 11 (left) and Eq. 14 (right).

4 CONCLUSIONS

A new hydraulic roughness equation has been derived for submerged vegetation. The equation relates the Manning roughness coefficient to the vegetation parameters (including flexibility), flow depth and a zero-plane displacement parameter. The equation is calibrated from the synthetic velocity profile data generated by a numerical model which has been extensively verified. A large number of experimental data by various investigators is then used to verify the equation and its simplified version. The performance of the equations is good and better than the previous equation without the zero plane displacement parameter. The equations have been subsequently applied to the field successively.

ACKNOWLEDGEMENT

This work is supported by the Research Grant Council of the Hong Kong Special Administrative Region under Grant No. 5200/12E and a grant from the Hong Kong Polytechnic University.

References

Baptist, M.J, Babovic, V, Keijzer, M, Uttenbogaard, R.E, Mynett, A and Verwey, A., 2007. On inducing equations for vegetation resistance. Journal of Hydraulic Research, Vol. 45, No. 4, pp 435 -450.

Bowmer, K.H, Jacobs, S.W.L and Sainty, G.R., 1995. Indentification, Biology and Management of Elodea canadensis,

Hydrocharitaceae. Journal of aquatic management. 33, 13-19.
Brian M. Stone, A.M. and Hung Tao Shen., 2002. Hydraulic Resistance of Flow in Channels with Cylindrical Roughness. Journal of Hydraulic Engineering, Vol. 128,No. 5, pp 500-506
Carollo, F.G, Ferro, V and Termini, D., 2002. Flow measurement in vegetated channels. Journal of Hydraulic Enginnering. Olume 128, number 7, pp 664-673.
Carollo, F.G., Ferro, V. and termini, D., 2005. Flow resistance law in channels with flexible submerged vegetation. Journal of Hydraulic Engineering, Vol.131, No.7. pp 554-564.
Gu Feng-feng., 2007. Roughness coefficients for unsubmerged and submerged reed. Journal of Hydrodynamics. Volume 19, number 4, pp 421-428.
Hofstra, D.E, Gemmill, C.E.C and Winton, M.D., 2006. Preliminary genetic assessment of New Zealand Isoetes and Nitella, using DNA sequencing and RAPDs. Science for Conservation 266.
Huai, W., Chen, Z. and Han, J., 2009. Mathematical model for the flow with submerged and emerged rigid vegetation. Journal of Hydrodynamics. Volume 21, number 5, pp722-729.
Ikeda, S and Kanazawa, M., 1996. Three dimensional organized vortices above flexible water plants. Journal of Hydraulic Engineering, Vol.122, No.11., pp 634-640.
Jarvela, J., 2005. Effect of submerged flexible vegetation on flow structure and resistance. Journal of Hydrology, 307, pp 233–241
Kevin, C., Johlene, K., and Paul, C., 2007. Regional guidelines for ecological assessments of freshwater environments: Aquatic plant cover in wadeable streams. Environment Waikato Technical report 2006/47.
Klopstra, D., Barneveld, H.J, Noortwijk, J.M and Velzen, E.H., 1997. Analytical model for hydraulic roughness of submerged vegetation. The 27th Congress of IAHR, San Francisco, 775-780.
Kouwen, N. and Unny, T.E., 1973. Flexible roughness in open channels. J. Hydraul. Div., ASCE, 99(5), 713-728.
Li, C.W and Xie, J.F., 2011. Numerical modeling of free surface flow over submerged and highly flexible vegetation. Advances in Water Resources, 34, 468–477.
Li, C.W and Zeng, C., 2009. 3D numerical modeling of flow divisions at open channel junctions with or without vegetation. Advances in Water Resources, 32, 46-60.
Lopez, F and Garcia, M.H., 2001. Mean flow turbulence structure of open-channel flow through non-emergent vegetation. Journal of Hydraulic Engineering, Vol.127, No.5., pp 392-402.
Nikora, V., Scott, L., Nina, N., Koustuv, D., Glenn, C. and Michael, R., 2008. Hydraulic resistance due to aquatic vegetation in small streams: Field study. Journal of Hydraulic Engineering, Vol.134, No.9., pp 1326-1332.
Poggi, D., Porporato, A., Ridolfi, L., Albertson, J. D and Katul ,G. G., 2004. The effect of vegetation density on canopy sub-layer turbulence. *Boundary-Layer Meteorology* 111: 565–587.
Raupach, M.R., 1994. Simplified expression for vegetation roughness length and zero-plane displacement as functions of canopy height and area index. Boundary Layer Meteorology, Volume 7, pp 211- 216.
Spalart, P. R., and Allmaras, S. R., 1994. A one-equation turbulence model for aerodynamic flows. La Recherche Aerospatiale, 1(1), 5-21.
Stephan, U and Gutknecht, D., 2002. Hydraulic resistance of submerged flexible vegetation. Journal of Hydrology 269, pp 27-43.
Velasco, D, Bateman, A. and Medina, V., 2008. A new integrated, hydro-mechanical model applied to flexible vegetation riverbeds. Journal of Hydraulic Reseach, Vol. 46, No. 5, pp 579-597.
Wilson, C.A.M.E, 2007. Flow resistance models for flexible submerged vegetation. Journal of Hydrology, 342, pp 213– 222.
Zeng, C., 2011. Numerical and experimental studies of flows in open channels with gravel and vegetation roughnesses. PhD thesis, Department of Civil and Structural Engineering, The Hong Kong Polytechnic University. 197pp.
Taka-aki, O and Nezu, I., 2010. Flow resistance law in open-channel flows with rigid and flexible vegetation. River Flow 2010.